Biological Mechanisms Revealed by a Mathematical Model for p53-Mdm2 Core Regulation

Yang YANG, Keem Swan LEE, Cheng XIANG, Hai LIN*

Department of Electrical and Computer Engineering

National University of Singapore, Singapore, 117576

{yang82, keemswan, elexc, elelh}@nus.edu.sg

March 26, 2009

Abstract

p53 is a paramount protein in cancer studies, and p53-Mdm2 interaction is the core regulation for most activities of p53 protein-related networks. In this paper, a new mathematical model is built to characterize the p53-Mdm2 interaction based on the recent biological findings, as well as a few reasonable hypotheses and approximations. ATM's dynamics is introduced to the model so as to connect DNA damage signal with the core regulation. The simulation results are in good accord with the experimental observations in the literature. More importantly, through bifurcation analysis on the model, a new threshold mechanism is predicted with respect to the dose of ionizing radiation (IR). Furthermore, a novel frequency shifting phenomenon is also observed through Fourier frequency analysis on the simulation data. Finally, based on the predicted dominant frequency, an optimized experimental scheme

*Corresponding author

is proposed to guide the experimental procedure. Once these two predicted mechanisms are validated through wet-lab experiments, they could provide us more insights for p53-Mdm2 core regulation and related pathways.

1   Introduction

The p53 tumour suppressor lies at the center of cellular pathways that sense DNA damage, cellular stress and oncogenetic stimulation [1]. p53 integrates such signals and, in response, induces growth arrest, triggers apoptosis (programmed cell death), blocks angiogenesis or mediates DNA repair, etc [2]. The critical role of p53 is experimentally evidenced by the presence of mutations found in almost 50% human tumours. Therefore, studies of p53 have attracted attentions of many researchers in life science for decades [3].

p53 serves as a transcriptional activator to promote the target genes' expressions and the downstream products will repair the double-strand breaks (DSB) and ultimately mitigate the DNA damage [4]. However, the p53 network is normally "off". In normal cells p53 protein usually maintains at a low level and has a short half-life due to the degradation by ubiquitination and proteolysis. The inhibitor is Mdm2 protein which is a E3 ubiquitin ligase for p53 and also a target gene of p53 simultaneously. Apparently, there exists a negative feedback to maintain the low p53 level. The core regulation can be simply represented as p53 $\rightarrow$ Mdm2 $\dashv$ p53. Furthermore, the Mdm2-interacting region in p53 resides at the 1-42 amino acids within N-terminal region. On the other hand, when the cell is stressed by DNA damage signal, such as ultraviolet (UV), ionizing radiation (IR), etc, ATM will add phosphate group to the serine 15 which leads to the poor binding ability of Mdm2 to p53. Thus the p53 level will be raised and activated to perform its major functions. Besides, ATM has another role to accelerate the transcription of target genes by phosphorylation

of p53 [5]. All the above introductions can be summarized in Fig. 1.

Recently, two research groups found the oscillation phenomena in p53-Mdm2 loop [6,7]. Damped oscillatory behaviors in population of cells and undamped oscillatory behaviors in individual cells were observed after the irradiation. Oscillatory expressions are actually observed in many other systems, such as Hes1 and NF-κB related networks [8–10]. Due to the lack of biological evidences and experimental data, the true mechanisms are not illustrated yet. Therefore, these oscillations motivate researchers' interest in the study of p53-Mdm2 core regulation; and many investigations have been devoted to build a reasonable model to qualitatively explain this oscillatory phenomenon.

It has been learned that oscillations can arise from negative feedback alone, which is composed of at least three components [11]. So in Lev Bar-Or's work [6], they resorted to a putative intermediary in the negative feedback loop. They explored the dependence of oscillations on different parameters, such as k_{delay}, which represents the time lag from intermediary to Mdm2. This inspired other research efforts which considered this time lag as an explicit parameter in the transcriptional and translational process of Mdm2. One of the representative studies was done by Monk in [8], where he proposed a delayed feedback model and integrated all the time lags as one explicit term in the formation process of Mdm2. From then on, most researchers have adopted this idea for modeling the p53-Mdm2 regulation, such as [12, 13]. In particular, Wagner and his coworkers took a significant step in investigating the global dynamics under different parameter bifurcations in [12]. An alterative approach was suggested in [14] by Tyson and his colleagues via introducing a positive feedback mechanism besides the common negative feedback loop, without relying on the explicit time delay.

Another remarkable work from Alon's research group gave a long-term (up to 3 days) experimental

data set in [15]. Moreover, they summarized six different model types for the dynamics of p53-Mdm2 network. They built a stochastic model concerning about the variability between cells as well. Other studies from a stochastic point of view were done in [16, 17]. Most recently, Ramalingam and his colleagues collected the experimental data using protein lysate microarrays [18]. Then based on the observations, they identified the parameters of the mathematical model adopted from [6, 16]. Subsequently, they knocked out p53 gene *in silico* by setting the production rate as zero. Finally, they made a good verification by the real experiment *in vivo*.

In this paper, the main objective is to investigate the p53-Mdm2 regulation in both time and frequency domains so as to obtain more insights on the regulatory mechanisms and propose verifiable hypotheses. First of all, a new mathematical model, which falls into the category of delayed feedback, is proposed by taking ATM's dual role into account. ATM is involved to associate the DNA damage signal with this core regulation, which is expressed by a simple dynamics in the model. Next, using this converter, bifurcation analysis of p53 with respect to ionizing radiation is performed; consequently, a threshold mechanism of radiation dose, which has never been discussed before, is found. Moreover, variation of p53-Mdm2 oscillation frequency is usually ignored in the existing literature. Inspired by this, we investigate frequency shifting phenomenon by Fourier frequency analysis on the model. Accordingly, we facilitate the experiment design by an optimized guideline. Bifurcation and frequency analysis are both contributing to the experimental validation and design in practice.

The rest of this paper is organized as follows. In Section 2, mathematical expressions are derived one by one according to the biological bases and assumptions. Next, simulation results and bifurcation analysis are given to exploit the model. In Section 4, through Fourier frequency analysis, a design scheme is provided to help conducting the wet-bench experiments. Discussion part is

4

dedicated to advise experimental verifications for model predictions. Finally, this paper ends with the conclusion part.

2 Formulation

Our model relies on prevailing evidences and widely accepted assumptions. For the sake of simplicity, only the p53 and Mdm2 proteins are considered, rather than the messenger RNAs of them. The reliability of this simplification will be verified by the later simulation results. The delays happened in the transcription, translation and translocation processes are all merged as one delay term appearing explicitly in the Mdm2 dynamics. The selections of parameters are performed after scaling the original equations.

2.1 Model

First of all, p53 dynamics is evaluated as

$$\frac{\mathrm{d}p53}{\mathrm{d}t} = a_p - d_p \times p53 - deg(S(t)) \times \frac{p53}{p53 + K_p} \times Mdm2. \tag{1}$$

Here the first term a_p specifies the synthesis rate of the p53 protein; the second term reflects the Mdm2-independent p53 degradation, while d_p is the basal degradation rate; the last term describes the Mdm2-induced p53 degradation. Michaelis-Menten kinetics is applied to this process, consistent with an enzyme (Mdm2)-catalyzed degradation from a substrate (p53 protein). As for $deg(S(t))$, it is the degradation rate which is a function of ATM, denoted by $S(t)$.

The expression for $deg(S(t))$ is

$$deg(S(t)) = d_0 \times (1 - \frac{S^n}{S^n + K_1^n}), \tag{2}$$

5

where d_0 is the basal rate for Mdm2-dependent p53 degradation. As shown in [5] , when the cell is exposed to the ionizing radiation, ATM can weaken the binding ability of Mdm2 to p53. So this basal degradation rate will be reduced by the existence of ATM. It is assumed that the reduction follows a Hill function with order, also called cooperativity, n.

Secondly, the dynamics of Mdm2 is described in the following equation,

$$\frac{\mathrm{d}Mdm2}{\mathrm{d}t} = a_m - d_m \times Mdm2 + agg(S(t)) \times \frac{p53^4(t-\tau)}{p53^4(t-\tau) + K_m^4}, \tag{3}$$

where the coefficients a_m and d_m give the basal rate of synthesis and degradation for Mdm2, respectively. The last term represents the transcription activation of Mdm2 by p53. Here transcription product— Mdm2 messenger RNA is replaced by Mdm2 protein and phosphorylated p53 is replaced by p53 protein. The two forms of p53 will not be discriminated in this model. The phosphorylation by ATM kinase is expressed in the coefficient function $agg(S(t))$. To account for p53's preference for tetramerisation [19], P2 promoter's dependence on p53 is modeled as a Hill function with cooperativity 4. Time lag τ is utilized to represent all the duration cost in this process.

The function $agg(S(t))$ is formulated as

$$agg(S(t)) = a_0 \times \frac{S^m}{S^m + K_2^m}, \tag{4}$$

Finally, the connection from stress signal to the core regulation via ATM's kinetics comprises the following two first-order dynamics.

$$\frac{\mathrm{d}S}{\mathrm{d}t} = k \times dam - d_s \times S. \tag{5}$$

$$\frac{\mathrm{d}dam}{\mathrm{d}t} = \frac{1}{T_1} \times (IR - dam). \tag{6}$$

Eq.(5) shows the ATM's dependence on the DNA damage denoted by dam, in which the second term describes the degradation of ATM. Eq.(6) describes damage generated due to ionizing radia-

6

tion *IR*, i.e. the input to the whole system. On the other hand, when the stress signal is withdrawn,

it is assumed that the repair of DNA damage will follow the process below.

$$\frac{\mathrm{d}dam}{\mathrm{d}t} = -\frac{1}{T_2} \times dam. \tag{7}$$

2.2 Selection of parameters

In this subsection, we introduce the following new variables and scaling relationships.

$$p\hat{5}3 = \frac{d_m}{a_p}p53, M\hat{d}m2 = \frac{d_m}{a_m}Mdm2, \hat{S} = \frac{d_m}{k}S$$

$$\hat{t} = d_m t, \hat{\tau} = d_m \tau$$

$$\hat{d}_p = \frac{d_p}{d_m}, \hat{K}_p = \frac{d_m}{a_p}K_p, \hat{K}_m = \frac{d_m}{a_p}K_m$$

$$\hat{d}_0 = \frac{a_m d_0}{d_m a_p}, \hat{a}_0 = \frac{a_0}{a_m}, \hat{T}_1 = \frac{1}{T_1 d_m}, \hat{T}_2 = \frac{1}{T_2 d_m}$$

$$\hat{d}_s = \frac{d_s}{d_m}, \hat{K}_1 = \frac{d_m}{k}K_1, \hat{K}_2 = \frac{d_m}{k}K_2$$

Here, we use dimensionless scaling to help reducing the burden for selection of parameters, which

is a common method in systems modeling [12, 20]. Thus, the rescaled dynamics is expressed by

the new variables in the following form.

$$\frac{\mathrm{d}p\hat{5}3}{\mathrm{d}\hat{t}} = 1 - \hat{d}_p \times p\hat{5}3 - deg(\hat{S}(\hat{t})) \times \frac{p\hat{5}3}{p\hat{5}3 + \hat{K}_p} \times M\hat{d}m2$$

$$\frac{\mathrm{d}M\hat{d}m2}{\mathrm{d}\hat{t}} = 1 - M\hat{d}m2 + agg(\hat{S}(\hat{t})) \times \frac{p\hat{5}3^4(\hat{t} - \hat{\tau})}{p\hat{5}3^4(\hat{t} - \hat{\tau}) + \hat{K}_m^4}$$

$$\frac{\mathrm{d}\hat{S}}{\mathrm{d}\hat{t}} = dam - \hat{d}_s \times \hat{S}$$

$$\frac{\mathrm{d}dam}{\mathrm{d}\hat{t}} = \frac{1}{\hat{T}_1} \times (IR - dam)$$

$$\frac{\mathrm{d}dam}{\mathrm{d}\hat{t}} = -\frac{1}{\hat{T}_2} \times dam, \text{ when stress signal is withdrawn}$$

7

$$deg(\hat{S}(\hat{t})) = \hat{d}_0 \times (1 - \frac{\hat{S}^n}{\hat{S}^n + \hat{K}_1^{\,n}})$$

$$agg(\hat{S}(\hat{t})) = \hat{a}_0 \times \frac{\hat{S}^m}{\hat{S}^m + \hat{K}_2^{\,m}}$$

To highlight the role of p53 in transcriptional activation, $\hat{a}_0$ should be selected much greater than 1, which is the unitized basal synthesis rate of Mdm2. The same selection criterion is applicable to the p53's degradation rates. Mdm2 makes the p53's proteolysis much faster compared with the basal degradation. Hence $\hat{d}_0$ is reasonably considered much greater than $\hat{d}_p$. In most existing literatures, the basal synthesis rate of Mdm2 and degradation rate of p53 are neglected. As for the Hill function's cooperativity, orders of 1 and 4 in Eq.(1) and Eq.(3) are selected according to the Michaelis-Menten kinetics and p53's tetramerisation. The orders of n and m used in Eq.(2) and Eq.(4) are determined by the sensitivity of the components. Moreover, the time delay τ is a key factor for the existence of oscillation [21]. For example, the values below a critical point $\tau_0 = 0.875$ will eliminate the oscillation when *IR* is set as 0.5 in this model.

Summarizing above, all the parameters are listed in Table 1. In the following, we omit the hat accent from the variables and parameters in the scaled equations and use *P* and *M* as abbreviations of p53 and Mdm2 respectively, as these changes do not cause misunderstandings.

3 Simulation and Bifurcation Analysis

3.1 Simulation Result

Our model exhibits sustained oscillation in response to increased radiation dose. As can be seen in Fig. 2, during the interval $0 \leq t \leq 15$, the cell stays under normal condition without exposure to ionizing radiation (*IR* = 0). p53 is maintained at low level due to the spontaneous inhibition by

Table 1: Parameter List of dimensionless kinetics equations

Parameter	Value	Parameter	Value
$\hat{d}_p$	0.2	$\hat{d}_0$	2
$\hat{K}_p$	0.2	$\hat{K}_1$	0.3
		$\hat{a}_0$	4
$\hat{K}_m$	0.5	$\hat{K}_2$	0.2
m	2	n	2
$\hat{\tau}$	1	$\hat{d}_s$	1
$\hat{T}_1$	2	$\hat{T}_2$	100

Mdm2. After $t > 15$, the cell is exposed to ionizing radiation ($IR = 0.5$). The oscillation persists until ionizing radiation is withdrawn at $t = 100$. Then the p53 and Mdm2 both return to the original states through a transient process, which consists of damped oscillations. It will be seen that the levels of p53 and Mdm2 differ much, which is due to the scaling operation. However, we will focus on the qualitative behavior rather than the quantitatively accurate time and concentration information in this work.

The first peak of p53 is earlier than Mdm2 after onset of IR, and the lag is about 1.8. The periods for both variables are the same. These performances fit to the experimental data in [6, 7] and previous simulation results. The difference resides on the scale, which is due to the parameters' selections. The evolvement also agrees with the observed experimental phenomenon.

After performing simulations under different dose levels, it is observed that the oscillation period is changing, although it is not very obvious in the time domain of simulation results using cur-

rent parameter set. This interesting variation inspires the detailed frequency analysis discussed in Section 4.

As evidenced by the experimental data shown in Fig.6b of [6], weak damage signal will slow the rise of steady state and no observable oscillations exist within the time frame of the experiment. To verify this point, IR is reduced to 0.2, and the result depicted in Fig. 3 shows that the oscillation disappears and settling time is elongated compared to the previous case.

3.2 Bifurcation Analysis

According to the simulation results above, during the sustained oscillation interval, when $IR = 0.2$, p53 stays at a stable steady state. When IR is raised to 0.5, p53 will oscillate, meaning that the original fixed point changes its stability. Moreover, if IR is considered as a parameter, it will induce the bifurcation of the nonlinear systems expressed by Eq.(1)–(6). Specifically, this is Hopf Bifurcation, i.e. the stable equilibrium point becomes unstable by a parameter change, and a limit cycle appears in the neighborhood [22].

Eq.(5) and (6) show the independence of S and dam on the p53 and Mdm2 dynamics. The solutions of $S(t)$ and $dam(t)$ are shown as

$$
\begin{aligned}
S(t) &= e^{-d_s t} S(0) + k \int_0^t dam(\tau) e^{-d_s(t-\tau)} d\tau \\
dam(t) &= e^{-t/T_1} dam(0) + IR \times T_1 \int_0^t e^{-T_1(t-\tau)} d\tau
\end{aligned}
$$

The settling times depend on the parameter d_s and T_1.

Meanwhile, given $d_s = 1$ and $T_1 = 2$, let

$$
\begin{aligned}
\frac{dS}{dt} &= dam - d_s \times S^* = 0 \\
\frac{d\,dam}{dt} &= \frac{1}{T_1} \times (IR - dam^*) = 0
\end{aligned}
$$

10

then get the steady-state equality $S^* = dam^* = IR$, where asterisk denotes the steady state. Therefore, in the given parameter set, the variables S and dam get equal to input IR fast.

Thus, it is convenient to study the bifurcation of reduced systems, which is comprised of only p53 and Mdm2 kinetics. Let the right hand sides of scaled p53 and Mdm2 equations equal zero and replace S with $S^* = IR$.

$$1 - d_p \times P^* - deg(IR) \times \frac{P^*}{P^* + K_p} \times M^* = 0 \tag{8}$$

$$1 - d_m \times M^* + agg(IR) \times \frac{P^{*4}}{P^{*4} + K_m^4} = 0 \tag{9}$$

After arrangement, by using the same parameter set above, an implicit function of P^* with the parameter IR is derived below.

$$1 - 0.2P^* - \frac{0.18}{IR^2 + 0.09} \times \frac{P^*}{P^* + 0.2} \left[1 + \frac{4IR^2}{IR^2 + 0.04} \times \frac{P^{*4}}{P^{*4} + 0.5^4} \right] = 0 \tag{10}$$

According to Descarte's rule of sign [23], it is assured to have real positive solution. Because of the high order existing in the implicit function, it is hard to get a close-form solution of P^*. By sampling IR's range $[0.1, 0.3]$ by interval of 0.02, we perform symbolic solver in Matlab iteratively. Several pairs of coordinates can be obtained. The negative real roots and complex roots are filtered because of the reality consideration. When $IR = 0.2$, the steady state of p53 is approximately 0.277, the same as shown in Fig. 3, which can also be seen in bifurcation diagram shown in Fig. 4.

According to the bifurcation diagram, when $IR > 0.32$, the oscillation happens. When $IR > 0.56$, the oscillation disappears and returns to the unique steady state again. Theoretically, it is because ATM's level also becomes bigger when IR is sufficiently large. p53's degradation by Mdm2's ubiquitination is largely inhibited by ATM. That's to say, the third term of Eq.(1) can be neglected. Consequently, p53 level will be definitely raised, and Mdm2 is also aggregating due

to the transcriptional activation by p53, leading the level higher than the basal level. Thus, p53 and Mdm2 will not be influenced by the ATM as much as in the oscillation region, and the core regulation is modified by the elimination of Mdm2's inhibition on p53. An example can be seen in Fig. 5. So far, there are no experimental data showing the response of big dose of ionizing radiation. The analysis based on this model predicts the retrieval of stable steady states at higher level.

4   Frequency Analysis and Experiment Design

The numerical simulations suggest the changes of p53-Mdm2 oscillation periods with respect to the level of IR. This is a very interesting phenomenon and has never been discussed from simulations of the core regulation to the best of the authors' knowledge. In the time domain, the changes of periods are hard to be detected given the existence of noises, which motivate us to consider this issue in the frequency domain. In the frequency spectrum, the dominant frequencies due to oscillations will appear as pulses, which can be distinguished from noise. However, the direct validation of this predicted frequency shifting phenomenon requires accurate measurements of the p53 and Mdm2 concentrations at a very high sampling rate, say 10 times measurements per hour. This seems to be an unreasonable expectation for the current wet-lab experiment techniques. To address this issue, we turn to frequency domain analysis, in particular Discrete Fourier Transform(DFT) and Fast Fourier Transform(FFT) [24]. The main purpose of frequency domain analysis is to determine the frequency at which p53 oscillates when the value of IR changes at a relatively lower requirement for the data measurements. Another advantage of dealing with the experiment design in the frequency domain is that the original frequency of the oscillation can be perfectly reconstructed in theory with limited sampled data. Based on Fourier analysis, the sam-

pling frequency and total sample points required for proper design of experiment can be selected such that in practice, the original time series on p53 concentration can be reconstructed perfectly from the sampled data points.

4.1   Frequency domain analysis

Our first task here is to determine the frequency of the p53-Mdm2 oscillations under a specified IR level from our numerical simulation, which is called a predicted frequency. This is achieved through doing DFT on the simulated time series data and analyzing it in the frequency domain.

To obtain the DFT of the time series of p53 concentration, Fast Fourier Transform (FFT) is performed on the simulation result in Matlab. The *IR* value is set to be non-zero for the whole simulation interval as only the region where sustained oscillations occur is of interest. The time domain simulation result under this setting is given in Fig. 6. Then, the first one-third of the time series obtained is truncated before the FFT so that only the oscillations with constant amplitude are considered. Besides, the solution given by numeric solver is not equally spaced in time, so it is needed to interpolate the solution and resample it at a regular interval before performing FFT. This will make sure that the signal is a valid input for the FFT routine [25].

Based on Nyquist sampling theorem, the sampling frequency is chosen as 1, which is much more than twice the different dominant frequencies (results shown later). Another parameter to be considered here is the number of sample points N. N is chosen to be as large as possible so that the frequency determined from DFT is more accurate.

The amplitude spectrum of the DFT of the time series of p53 concentration when *IR* is set to 0.5 is shown in Fig. 7. There are two prominent peaks observed at $F = 0$ and $F = 0.1996$. The peak at $F = 0$ arises because there is a DC offset in the waveform. The peak at $F = 0.1996$

13

gives the dominant frequency of oscillation. The process was repeated for *IR* in oscillatory range [0.32, 0.56]. The frequencies of oscillation corresponding to different radiation doses are shown in Table 2.

Table 2: Normalized frequencies of oscillations for different *IR* values

IR	Frequency	*IR*	Frequency
0.33	0.2133	0.45	0.2045
0.36	0.2114	0.48	0.2016
0.39	0.2094	0.51	0.1986
0.42	0.2065	0.55	0.1937

From the spectral analysis, simulated results show that the maximum frequency of oscillation is 0.2133, which occurs at *IR* = 0.33. The minimum frequency of oscillation is 0.1937, which occurs at *IR* = 0.55, around the upper bound. Beyond these boundary *IR* values, no dominant peak can be observed in the amplitude spectrum, reflecting the fact that there is no sustained oscillation. Within the oscillatory region, we observe a monotonical decrease of the frequency when IR level increases. This is consistent with the observation in the time domain simulation which shows that the period increases when *IR* value increases. To confirm this, the DDE-BIFTOOL [26] is used to obtain a plot of period of oscillation against *IR* values as shown in Fig. 8, whose result is consistent with our frequency analysis. In [15], the authors stated that the period of oscillations did not appear to significantly depend on irradiation level. As investigated here, the period correlates to the IR dose. Therefore, more explorations need to be carried out.

4.2 Experiment Design

Based on the above analysis, a frequency shifting phenomenon is predicted by the mathematical model. As stated earlier, one purpose of performing frequency analysis is that it will help to determine the number of samples (N) and sampling frequency (F_s) necessary in the practical experiment such that the original signal is not distorted. N determines the total number of data points needed to sample the concentration of p53 while F_s determines how frequent the measurements need to be made. By optimally selecting N and F_s, much cost and time can be saved for carrying out the verifying experimental design. Here, we do not intend to adopt the optimization formulation, such as linear or nonlinear programming, as introduced in [27].

For DFT operation, perfect reconstruction of the original time domain signal from the discrete time samples requires $k = N\frac{F_0}{F_s}$ to be an integer where F_0 denotes the dominant frequency in the input signal. This is to guarantee that the DFT result can represent the original signal perfectly in the frequency domain. Else, the frequency domain representation is only an approximation of the original signal. Bearing this in mind, the method proposed here is to fix F_s as an integer multiple of F_0, e.g. $F_s = 3F_0$. N can then be chosen as any multiple of 3 and k will always be an integer. In other words, as few as 3 samples are required to obtain the frequency domain representation of the p53 concentration theoretically. In fact, this is an ideal case because the Nyquist frequency merely gives the lower bound of the sampling frequency. In practice, we usually need higher frequency than that. In this way, the DFT condition can be satisfied while the time and cost of conducting the verifying experiment can be minimized.

With the previous simulation result, the predicted frequency F_0 with respect to different IR values can be obtained. Hence corresponding F_s can be calculated. Herein one thing to note is that F_0 obtained in the simulation may not be the same as the actual frequency of oscillation obtained

in experiment. Therefore, further adjustments of F_s and N might be needed in practice since the model presented here is more of qualitative nature. However, the method presented here can be employed directly as guidelines of designing experiments provided that a reasonably reliable mathematical model is built. Therefore, a suggested experiment procedure could be designed as follows.

1. Build a quantitative-reliably enough mathematical model from more available datasets

2. Select the stable oscillatory simulated data to be dealt with by Matlab routine FFT, and identify the dominant predicted frequency F_0

3. When performing the experiment, measure the concentrations of p53 and Mdm2 every T ($= \frac{1}{n \times F_0}$, where $n = 4, 5 \ldots$) time after entering the steady oscillation stage

4. Collect N ($= k \times n$, where $k = 2, 3, \ldots$) numbers of data points in total

5. Reconstruct the actual oscillation including amplitude and frequency information from the collected data points after filtering the noise signal

5 Discussion

The threshold mechanism discovered by the bifurcation analysis has not been verified by the current experimental data so far. Hence, a verifying experiment is suggested to be conducted. Once the experiment is done, two scenarios may occur. On one hand, if a higher steady state of p53 is observed, which coincides with the prediction from the model, the model is validated, revealing true mechanisms in the core regulation to some extent. On the other hand, if the observation shows that there are still sustained p53 oscillations or low level of stable steady state, then we have to

refine or revise our current model. More aspects, such as the downstream activities of p53, which are involved in cell cycle, apoptosis and detailed DNA repair process [2], may have to be considered to improve the model's reliability, or, the role of ATM should be reevaluated to modify the interactions with the core regulation.

Regarding the frequency analysis, the predicted frequencies are normalized by the sampling frequency and converted from dimensionless time factor. According to Table 2, we can easily discriminate the differences in the frequency domain, and the practical measurement period usually takes several hours to days. Therefore, it is believed that the differences in the time domain are considerable in reality.

Furthermore, the real dominant frequency of p53 oscillations awaits more experimental data to be determined precisely. This real frequency will help to improve the model and design the experimental procedure. First, it can be utilized to refine parts of time-related parameters, such as degradation rate, repairing rate, etc. Secondly, with the knowledge of real frequency, it can replace the step 1 and 2 of the experimental procedure mentioned in Section 4.2. The following steps could get along directly without the help of mathematical model. Moreover, the concentration information is necessary for accurate reconstruction in practice. At this point, measurement techniques need to be improved to accomplish this.

Admittedly, with the existence of the inevitable noises and fluctuations under current technical status, the guideline provided is somewhat conceptual, still requiring further fine tuning and modifications with respect to practical considerations, such as noise filtering, statistical data processing, etc. Handling the noise is an open question in quantitative systems modeling. There are several ways for noise reduction besides the statistical inference of data. First of all, technical improvements help to make high-precision measurements [28]. Secondly, considering the variability be-

tween cells, stochastic modeling methods will comply with the natural essence more compared to deterministic modeling [29]. Thirdly, it is required to develop method to position the noise origin [30] and use specific mechanisms to lower the noise impact [31]. Therefore, it is a long way to fully develop quantitative computational biology.

In the current model, the variable *dam*, representing DNA damage, helps to resemble the damped oscillation after irradiation. The simulation results show that the magnitude of oscillations will monotonically decrease after the impulsive stimulus of irradiation, which depends on the degradation time constant T_2 in Eq.(7). Without the variable *dam*, the ATM's influence will fast disappear through a decaying dynamics, i.e. the oscillation will not persist for a long duration, which violates the common observations. Besides, ATM is expressed as the independent variable of Hill function in Eq.(2) and Eq.(4). The selection of K_1 and K_2 plays an important role for the tuning effects of ATM, which need to give enough tuning range for ATM. Otherwise, ATM will become dispensable.

To emphasize again, our main focus here is to develop a predictive mathematical model such that it recaptures the observations and provides new insights. So far, the model is a scaled version and semi-quantitative, and the parameters are mostly estimated by approximations or trial-and-error. This is due to the lack of quantitative reliable experimental data, such as the real-time concentrations. Our emphasis is to determine which variables to be included and identify their relationships than the precise values [32]. Once new data become available, the model can be refined and make more accurate predictions.

6   Conclusion

In this paper, a new mathematical model was proposed to explain the inherent mechanisms in p53-Mdm2 core regulation in response to DNA damage. The main structure was built in delayed differential equations. The simulation environment was in Matlab mainly using dde23 [33]. Selections of parameters and simplification assumptions were proven qualitatively appropriate by the good agreement of simulation results with the experimental phenomena.

In addition, a more detailed investigation was performed to analyze the bifurcation of p53's concentration with respect to the dose of ionizing radiation to predict a new threshold mechanism used to explore this core regulation. Meanwhile, the phenomenon of frequency shifting was observed from the simulation results. To help discriminating different frequencies, Fourier frequency analysis was applied to transform the oscillations in the time domain to distinct pulses in the frequency domain. Furthermore, based on the dominant frequency identified, an experiment procedure was provided to give suggestion on sampling frequency and data point number for the wet lab.

7   Acknowledgments

References

[1] Vogelstein, B., Lane, D. and Levine, A. J.:'Surfing in p53 network', Nature, 2000, 408, pp. 307-310

[2] Harris, S. L., and Levine, A. J.:'The p53 pathway: positive and negative feedback loops', Oncogene, 2005, 24, pp. 2899-2908

[3] Bourdon, J. C., Laurenzi V. D., Melino G., and Lane D.:'p53: 25 years of research and more questions to answer', Cell Death and Differentiation, 2003, 10, pp. 397-399

[4] El-Deiry, W. S.:'Regulation of p53 downstream genes', Seminars in CANCER BIOLOGY, 1998, 8, pp. 345-357

[5] Banin, S., Moyal, L., Shieh, S., Taya, Y., Anderson, C.W., and Chessa, L.:'Enhanced phosphorylation of p53 by ATM in response to DNA damage', Science, 1998, 281(5383), pp. 1674-1677

[6] Lev Bar-Or, R., Maya, R., Segel, L. A., Alon, U., Levine, A. J., and Oren, M.:'Generation of oscillations by the p53-Mdm2 feedback loop: a theoretical and experimental study', Proceedings of the National Academy of Sciences USA, 2000, 97(21), pp. 11250-11255

[7] Lahav, G., Rosenfeld, N., Sigal, A., Geva-Zatorsky, N., Levine, A. J., Elowitz, M. B., and Alon, U.:'Dynamics of the p53-Mdm2 feedback loop in individual cells', Nature Genetics, 2004, 36(2), pp. 147-150

[8] Monk, N. A.:'Oscillatory Expression of Hes1, p53 and NF-κB Driven by Transcriptional Time Delays', Current Biology, 2003, 13, pp. 1409-1413

[9] Nelson, D.E., Ihekwaba, A.E.C., Elliott, M., Johnson, J.R.,Gibney, C.A., Foreman, B.E., Nelson, G., See, V., Horton, C.A., Spiller, D.G., Edwards, S.W., McDowell, H.P., Unitt, J.F., Sullivan, E., Grimley, R., Benson, N., Broomhead, D., Kell, D.B., White, M.R.H. :'Oscillations in NF-κB Signaling Control the Dynamics of Gene Expression', Science, 2004, 306(5696), pp. 704-708

[10] Schmidt, H., and Jacobsen, E. W.:'Linear systems approach to analysis of complex dynamic behaviours in biochemical networks', IEE Systems Biology, 2004, 1(1), pp. 149-158

[11] Tyson, J. J., Chen, K. C., and Novak, B.:'Sniffers, buzzers, toggles and blinkers: dynamics of regulatory and signaling pathways in the cell', Current Opinion in Cell Biology, 2005, 15, pp. 221-231

[12] Wagner, J., Ma,L., Rice, J. J., Hu, W., Levine, A. J., and Stolovitzky, G. A.:'p53-Mdm2 loop controlled by a balance of its feedback strength and effective dampening using ATM and delayed feedback', IEE Systems Biology, 2005, 152(3), pp. 109-118

[13] Samuel, B., and Basile, G.:'Analysis of a minimal model for p53 oscillations', Jounal of Theretical Biology, 2007, 249, pp. 235-245

[14] Ciliberto, A., Novak, B., and Tyson, J. J.:'Steady States and Oscillations in the p53/Mdm2 Network', Cell Cycle, 2005, 4(3), pp. 488-493

[15] Geva-Zatorsky, N., Rosenfeld, N., Itzkovitz, S., Milo, R., Sigal, A., Dekel, E., Yarnitzky, T., Liron, Y., Polak, P., Lahav, G., and Alon, U.:'Oscillations and variablity in the p53 system', Molecular Systems Biology, 2006, 2006.0033

[16] Ma, L., Wagner, J., Rice, J.J., Hu, W., Levine, A.J., Stolovitzky G.A.:'A plausible model for the digital response of p53 to DNA damage', Proceedings of the National Academy of Sciences USA, 2005, 102, pp. 14266-14271

[17] Proctro, C.J., Gray, D.A.:'Explaining oscillations and variablity in the p53-Mdm2 system', BMC Systems Biology, 2008, 2(75)

[18] Ramalingam, S., Honkanen, P., Young, L., Shimura, T., Austin, J., Steeg P.S. and Nishizuka S.:'Quantitative Assessment of the p53-Mdm2 Feedback Loop Using Protein Lysate Microarrays', Cancer Research, 2007, 67(13), pp. 6247-6252

[19] Weinberg, R. L., Veprintsev, D. B., and Fersht, A. R.:'Cooperative binding of tetrameric p53 to DNA', Journal of Molecular Biology, 2004, 341(5), pp. 1145-1159

[20] Aguda, B.D., Kim, Y., Piper-Hunter, M.G., Friedman, A. and Marsh, C.B.,:'MicroRNA regulation of a cancer network: Consequences of the feedback loops involving miR-17-92, E2F, and Myc', Proceedings of the National Academy of Sciences USA, 2008, 105(50), pp. 19678-19683

[21] Nikolov, S., Vera, J., Kotev, V., Wolkenhauer, O., Petrov, V.:'Dynamic properties of a delayed protein cross talk model', BioSystems, 2008, 91, pp. 51-68

[22] Strogatz, S. H.:'Nonlinear Dynamics and Chaos, with Application to Physics, Biology, Chemistry, and Engineering'(Addison-Wesley, 2004)

[23] Korn, G., Korn, T.:'Mathematical Handbook for Scientists and Engineers' (McGraw-Hill Book Company, 1968)

[24] Oppenheim, A. V., Willsky, A. S., and Nawab, S. H.:'Signals and Systems' (Prentice-Hall, 2nd edn. 1997)

[25] http://www.mathworks.com/access/helpdesk/help/techdoc/ref/fft.html

[26] Engelborghs, K. , Luzyanina, T., and Samaey, G.:'DDE-BIFTOOL v. 2.00: a Matlab package for bifurcation analysis of delay differential equations', Technical Report TW-330, Department of Computer Science, K.U.Leuven, Leuven, Belgium, 2001 Banga and

[27] Balsa-Canto, E., Alonso, A. A.,Banga, J. R.:'Computational procedures for optimal experi-mental design in biological systems', IET Systems Biology, 2008, 2(4), pp. 163-172

[28] Newman, J. R. S., Ghaemmaghami, S., Ihmels, J., Breslow, D. K., Noble, M., DeRisi, J. L., and Weissman J. S.:'Single-cell proteomic analysis of S. cerevisiae reveals the architecture of biological noise', Nature, 2006, 441, pp. 840-846

[29] Lindner, B.:'Some unsolved problems relating to noise in biological systems', Journal of Statistical Mechanics: Theory and Experiment, 2009, doi: 10.1088

[30] Bar-Even, A., Paulsson, J., Maheshri, N., Carmi, M., O'Shea, E., Pilpel, Y. and Barkai, N.:'Noise in protein expression scales with natural protein abundance', Nature Genetics, 2006, 38(6), pp. 636-643

[31] Paulsson J.:'Prime movers of noisy gene expression', Nature Genetics, 2005, 37(9), pp. 925-926

[32] Wolkenhauer, O., Ghosh, B. K., and Cho, K. H.:'Control and Coordination in Biochemical Networks', IEEE Control Systems Magazine, 2004, 24(4), pp. 30-34

[33] Kierzenka, J., Shampine, L. F., and Thompson, S.:'Solving Delay Differential Equations with DDE23', available at `http://www.mathworks.com/dde_tutorial`
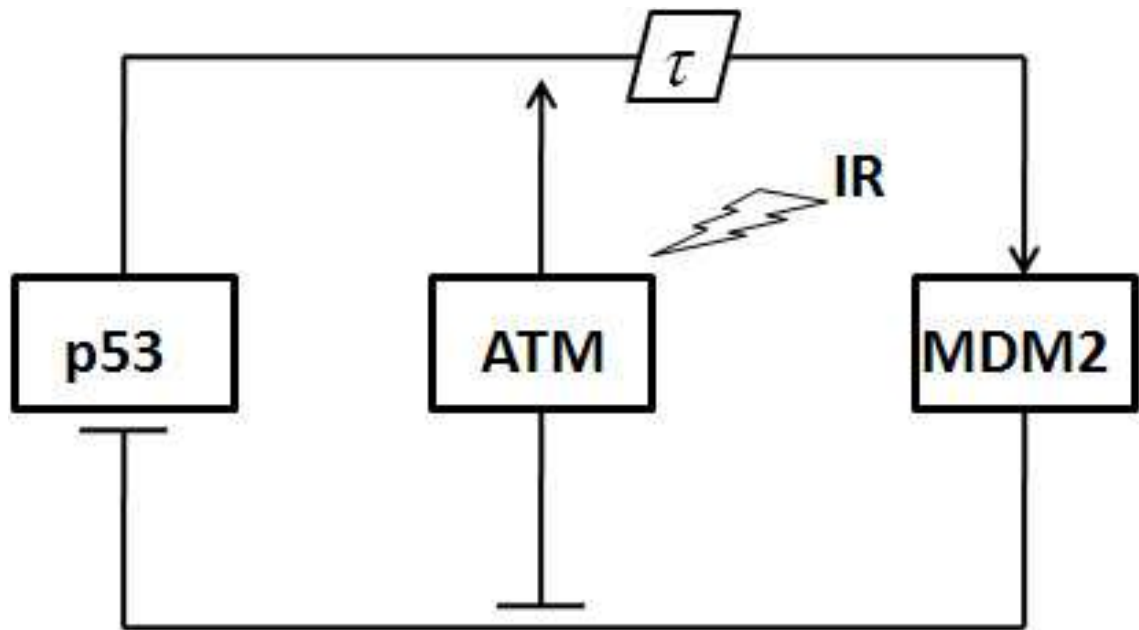
Figure 1: Schematic diagram to illustrate p53-Mdm2 core regulation. Arrow represents activation, while arrow-bar means inhibition. IR is short for ionizing radiation. τ is the assumed time lag from p53 to Mdm2's translation.
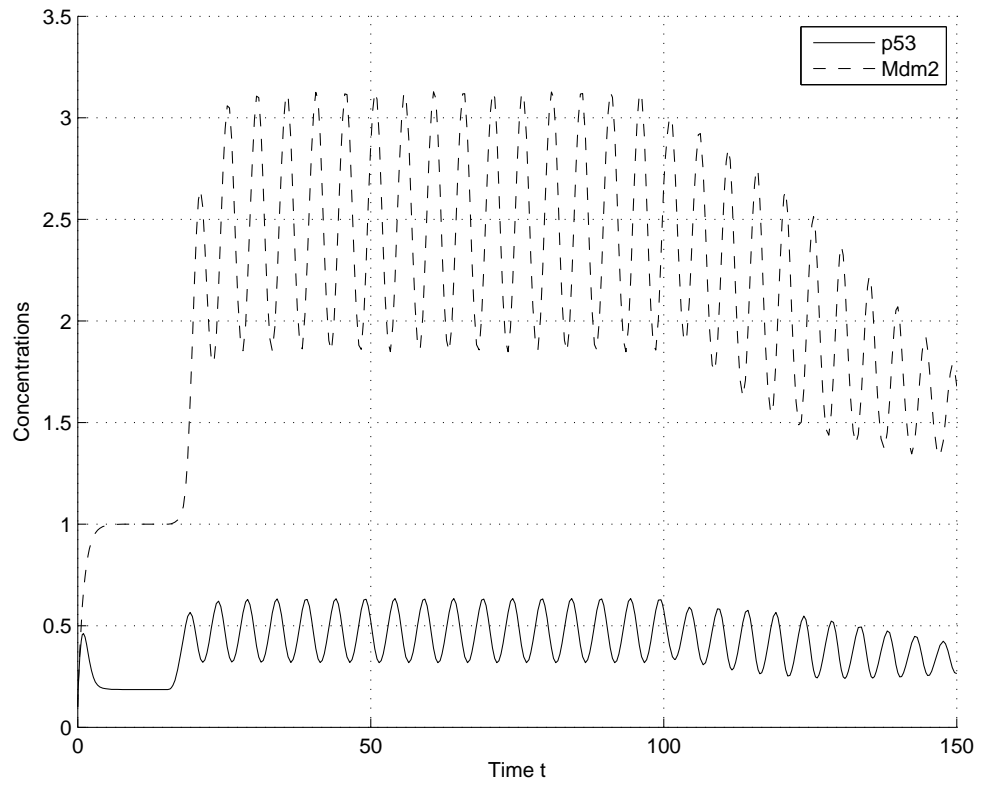
Figure 2: Temporal performances of p53 and Mdm2. During $15 \leq t \leq 100$, $IR = 0.5$. In other durations, $IR = 0$. Other parameters are listed in Table 1.
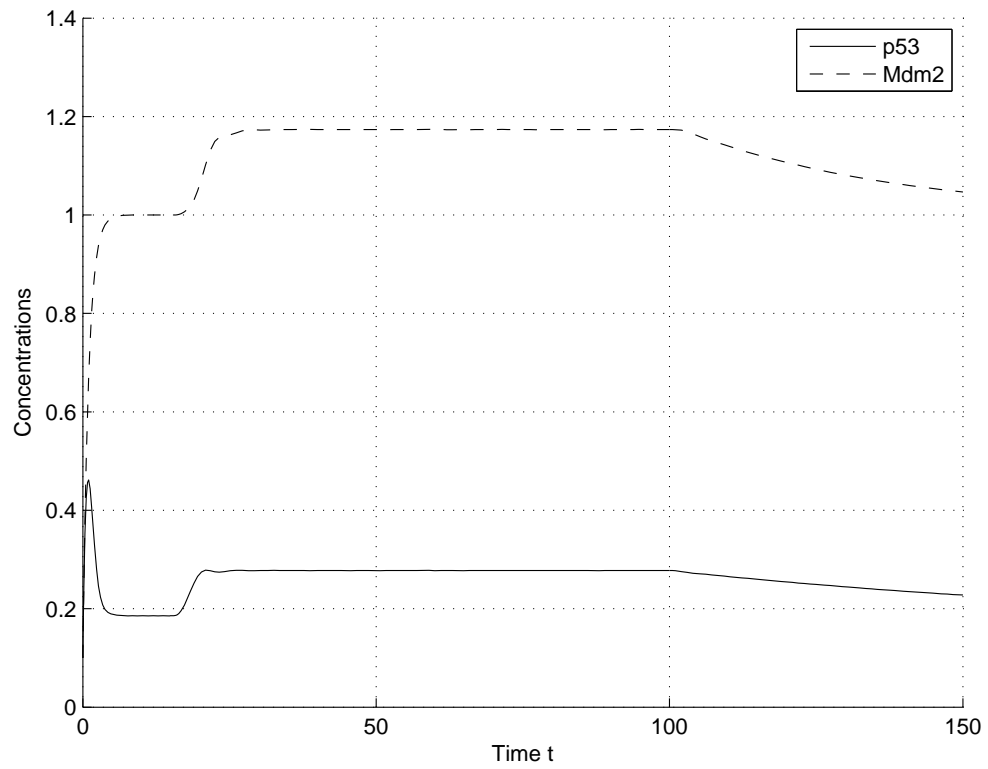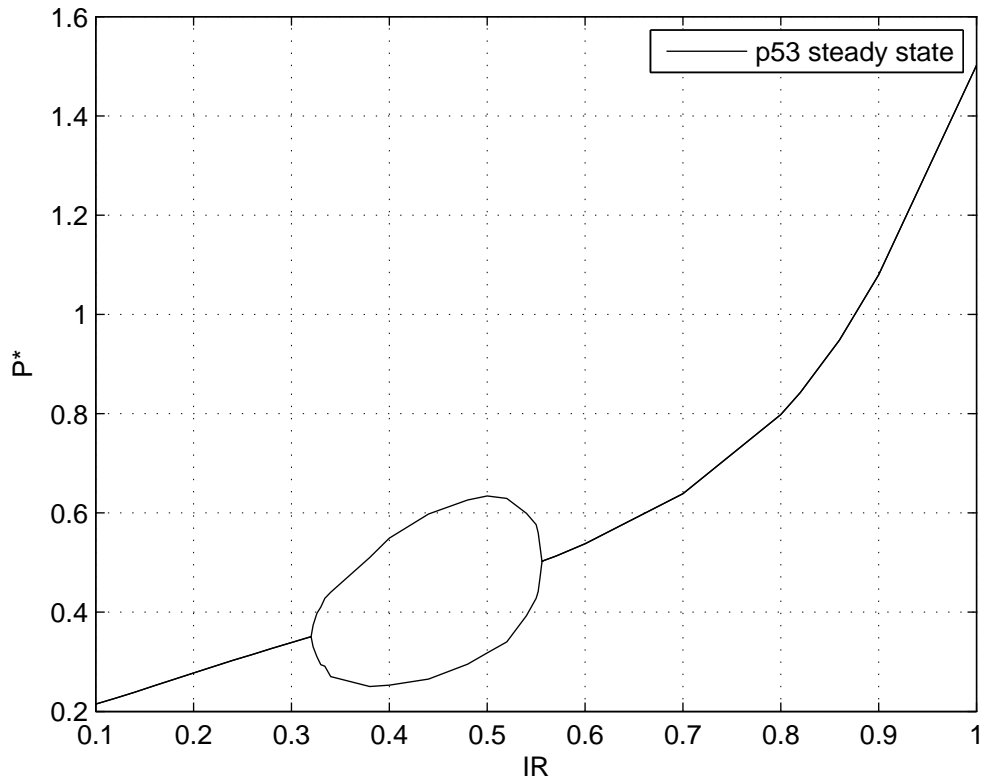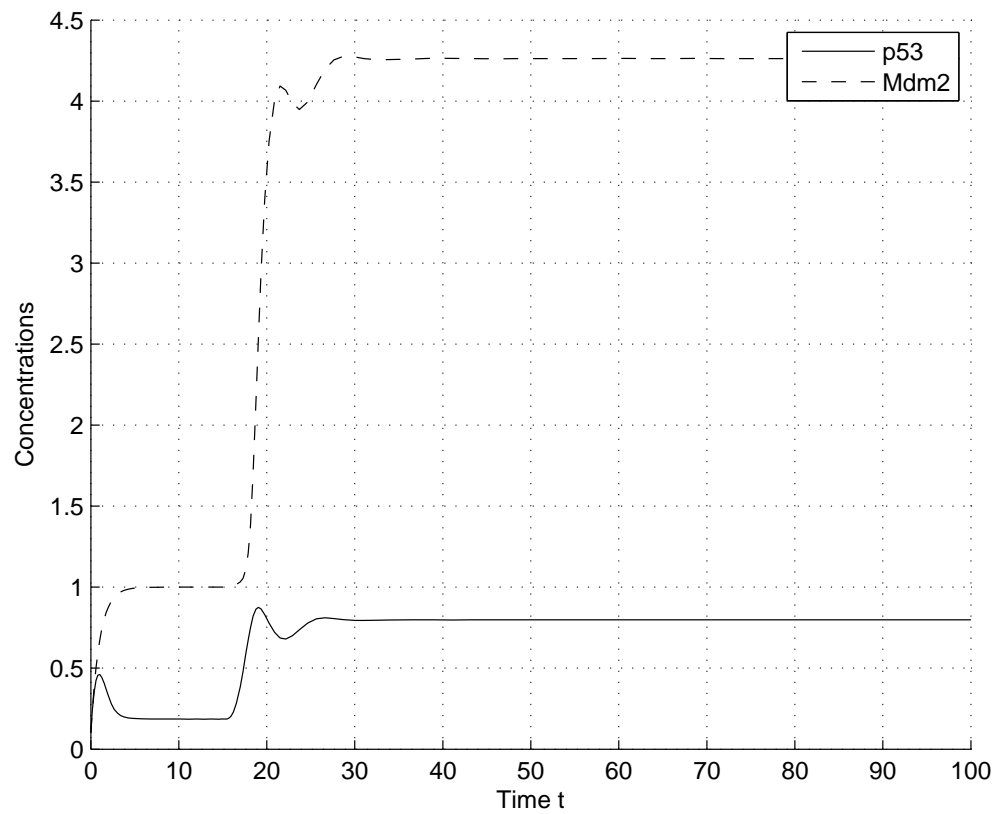
Figure 3: Temporal performances of p53 and Mdm2. During $15 \leq t \leq 100$, $IR = 0.2$. In other durations, $IR = 0$. Other parameters are listed in Table 1.

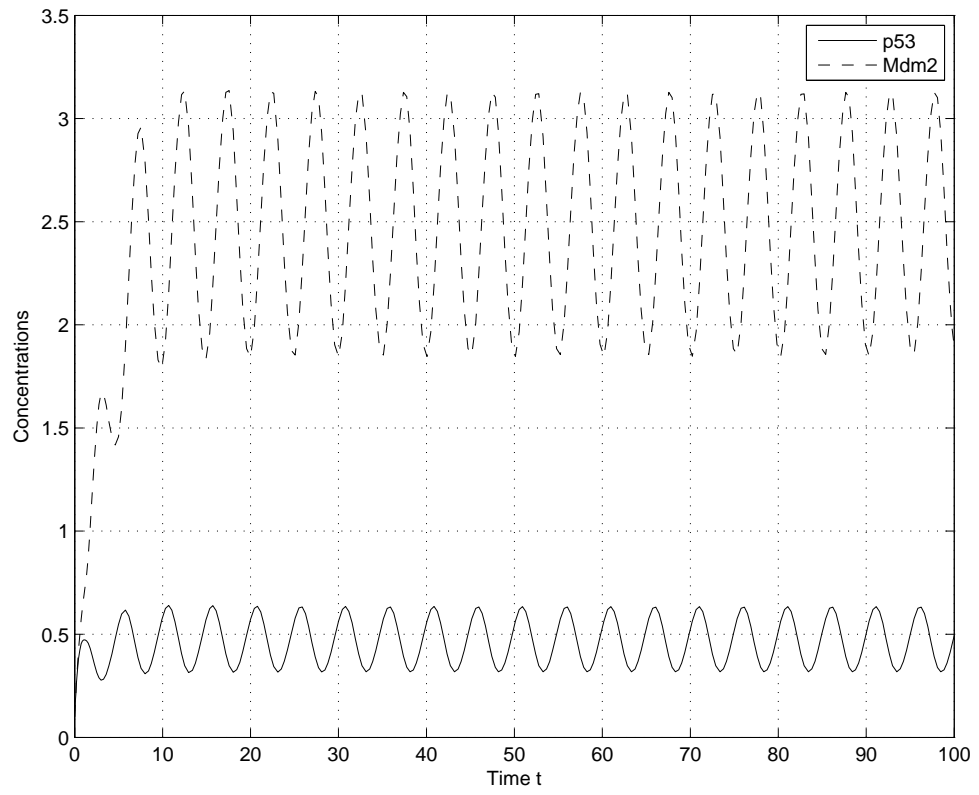Figure 4: Bifurcation diagram of p53's steady state with respect to *IR*. For the stable limit cycle, the maxima and minima are drawn. When *IR* is greater than 20, the steady state converges to 5. Data are not shown here.

Figure 5: Temporal performances of p53 and Mdm2. During $15 \leq t \leq 100$, $IR = 0.8$. In other durations, $IR = 0$. Other parameters are listed in Table 1.

Figure 6: Time domain simulation result with oscillation for whole time interval, *IR* = 0.5
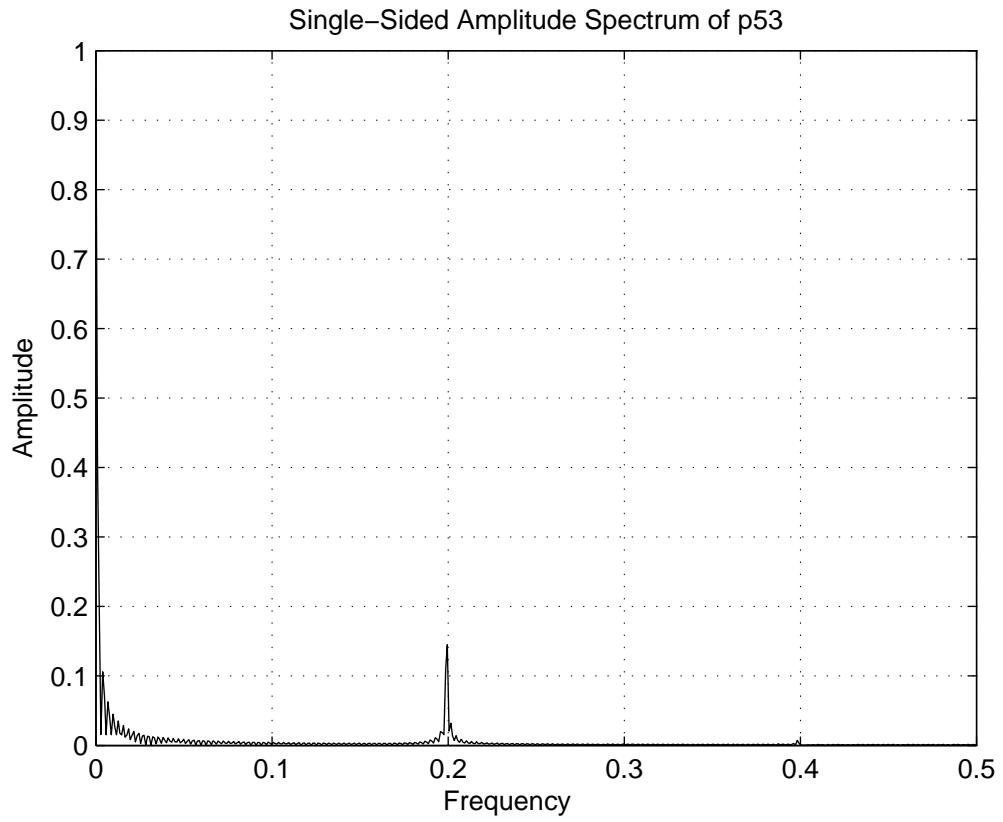
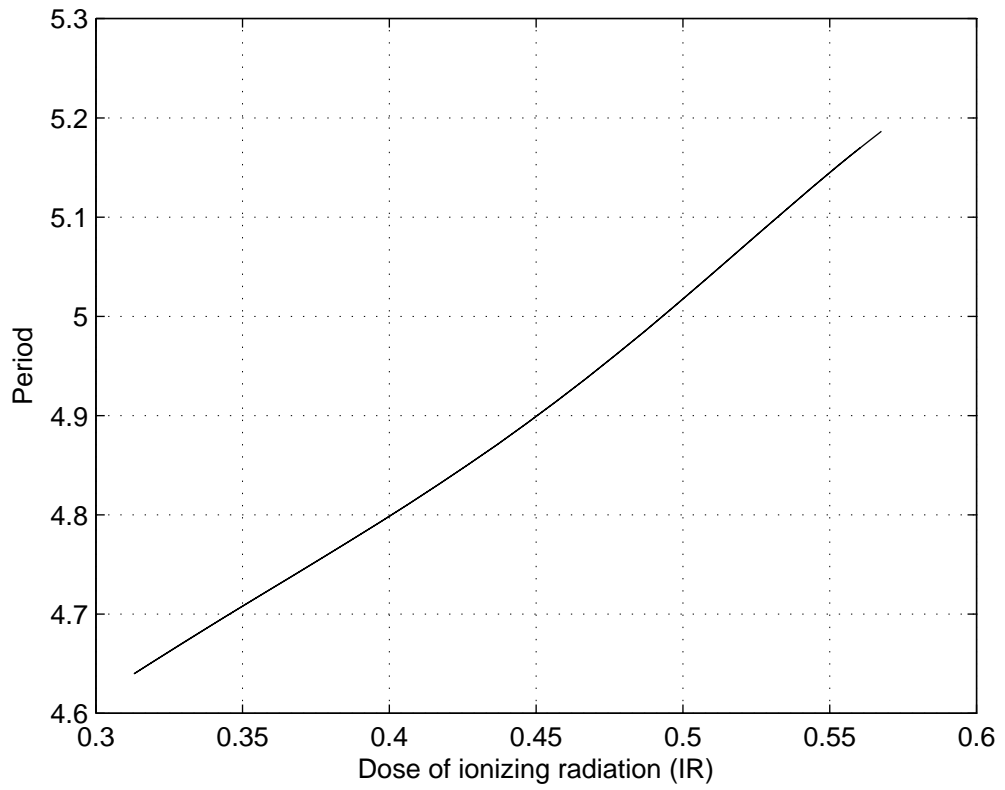Figure 7: Amplitude spectrum of DFT of p53 concentration when *IR* = 0.5

Figure 8: Periods of oscillations against different *IR* values analyzed by DDE-BIFTOOL [26]